Carbon Atoms in Ethanol Do Not Contribute Equally to Formation of Single-Walled Carbon Nanotubes

Rong Xiang,[†,*] Bo Hou,[‡] Erik Einarsson,[‡,§] Pei Zhao,[‡] Sivasankaran Harish,[‡] Kenichi Morimoto,[‡] Yuhei Miyauchi,[⊥,¶] Shohei Chiashi,[‡] Zikang Tang,[†,#] and Shigeo Maruyama[‡,*]

[†]State Key Laboratory of Optoelectronic Materials and Technologies, School of Physics and Engineering, Sun Yat-Sen University, Guangzhou 510275, China, [‡]Department of Mechanical Engineering and [§]Global Center of Excellence for Mechanical Systems Innovation, The University of Tokyo, 7-3-1 Hongo, Bunkyo-ku, Tokyo 113-8656, Japan, [⊥]Institute of Advanced Energy, Kyoto University, Uji, Kyoto 611-0011, Japan, [¶]PRESTO, Japan Science and Technology Agency, Kawaguchi, Saitama 332-0012, Japan, and [#]Department of Physics, Hong Kong University of Science and Technology, Clear Water Bay, Hong Kong, China

ABSTRACT We propose a unique experimental technique in which isotopically labeled ethanol, *e.g.*, $^{12}CH_3-^{13}CH_2-OH$, is used to trace the carbon atoms during the formation of single-walled carbon nanotubes (SWNTs) by chemical vapor deposition (CVD). The proportion of ^{13}C is determined from Raman spectra of the obtained SWNTs, yielding the respective contribution of ethanol's two different carbon atoms to SWNT formation. Surprisingly, the carbon away from the hydroxyl group is preferably incorporated into the SWNT structure, and this preference is significantly affected by growth temperature, presence of secondary catalyst metal species such as Mo, and even by the substrate material. These experiments provide solid evidence confirming that the active carbon source is not limited to products of gas-phase decomposition such as ethylene and acetylene, but ethanol itself is arriving at and reacting with the metal catalyst particles. Furthermore, even the substrate or other catalytically inactive species directly influences the formation of SWNTs, possibly by changing the local environment around the catalyst or even the reaction pathway of SWNT formation. These unexpected effects, which are inaccessible by conventional techniques, paint a clearer picture regarding the decomposition and bond breaking process of the ethanol precursor during the entire CVD process and how this might influence the quality of the obtained SWNTs.

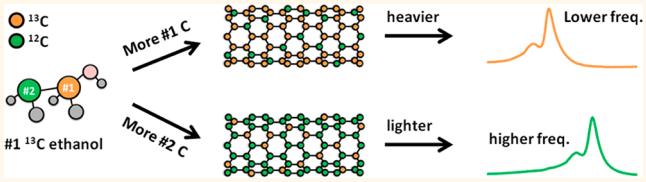

KEYWORDS: single-walled carbon nanotube · growth mechanism · isotope labeling · precursor decomposition

The catalytically driven formation of carbon nanotubes (CNTs) and graphene in the chemical vapor deposition (CVD) process usually involves catalyst particles/films, catalyst supports/substrates, and carbon sources.[1−4] Even only for CNTs, there are extensive explorations into the many combinations of these parameters, and the obtained materials have proven to be strongly dependent on these experimental parameters.[5−9] Taking the catalyst as an example, transition metals such as Fe, Ni, Co, and their combinations are known to be most successful in terms of CNT yield.[7] Stabilizing these active metals by subsidiary metal species, for example, Mo, tends to immobilize the transition metal, reducing the size of the catalyst and avoiding the oxidation of active catalyst, leading to the formation of single-walled carbon nanotubes (SWNTs).[10−14] This principle of bimetallic catalyst has been successfully demonstrated in the CoMoCAT[15] and alcohol catalytic CVD (ACCVD) processes,[14,16] where Co/Mo are preferentially used as the catalyst. A similar strategy applies to catalyst support, where Al oxide is found to be efficient in constraining the aggregation of iron and thus producing SWNTs with high yield and selectivity.[17−20] However, these understandings are largely based on empirical summaries, while the detailed formation process from a carbon-containing molecule to the final SWNT is generally treated as a black box. We understand that part of the reason for this is the lack of effective experimental strategies to monitor this complicated heterogeneous catalysis process.

Ethanol is one of the most widely used carbon sources for the synthesis of SWNTs. Various morphologies, including random networks, vertically aligned arrays, horizontally

* Address correspondence to xiangr2@mail.sysu.edu.cn, maruyama@photon.t.u-tokyo.ac.jp.

Received for review November 6, 2012 and accepted March 4, 2013.

Published online March 04, 2013
10.1021/nn305180g

aligned arrays, *etc*., have been successfully obtained using ethanol.[14,16,21,22] Different from other carbon sources like methane, ethylene, and acetylene, one unique feature of ethanol is that each molecule contains two inequivalent carbon atoms. An interesting proposition that arises from this asymmetric structure is whether or not both carbon atoms are incorporated into the final SWNTs. The answer to this question may be related to the stability of ethanol molecules in the gas phase and the bond breaking behavior on the catalyst surface. Finding an answer to this question becomes more meaningful after the molecular beam experiments by G. Eres *et al*. in which they identified acetylene as possibly the most efficient hydrocarbon for CNT growth by providing one molecule at a time, thereby avoiding thermal decomposition.[23,24] This experiment initiated further discussion on the activity of acetylene and the speculation that acetylene may be the actual precursor directly interacting with the catalyst clusters.[25−27] Since ethanol decomposes into ethylene and at high temperature further into acetylene, in this work we attempt to shed some light on the black-box process of SWNT formation from ethanol. We propose an experimental strategy using isotopically modified ethanol to trace the incorporation of ethanol's inequivalent carbons to SWNT formation. We find that the carbon away from the hydroxyl group is preferably incorporated into the final SWNTs (up to 85% in some cases), and the imbalance of carbon incorporation is significantly affected by CVD parameters and catalyst/substrate composition. These solid experimental data not only unambiguously confirmed the direct interaction between ethanol (the only asymmetric molecule) and catalyst, but also indicate that previously considered inactive species (such as catalytically inactive metals or oxide, see Supporting Information) can significantly influence the synthesis reaction process and strongly affect the properties of the produced SWNTs. These preliminary findings, together with calculations of the gas-phase thermal decomposition of the carbon source, enable a better understanding of the ethanol molecule's journey during the CVD process and how it affects the quality of produced SWNTs.

Decomposition of Ethanol and Possible Precursors for SWNT Growth. The CVD formation process of carbon nanotubes is not necessarily the direct interaction between the catalyst and the originally provided precursor, since hydrocarbon or alcohol molecules may decompose at high temperature before reaching the catalyst sites. Some of the carbon-containing molecules produced by this thermal decomposition are known also to be efficient for SWNT growth. In the case of ethanol, we have confirmed previously that ethanol quickly decomposes above 800 °C, primarily producing ethylene and water (see Supporting Information, Figure S1). Trace amounts of CO, methanol, and acetylene are also identified. For example, calculations suggest that when

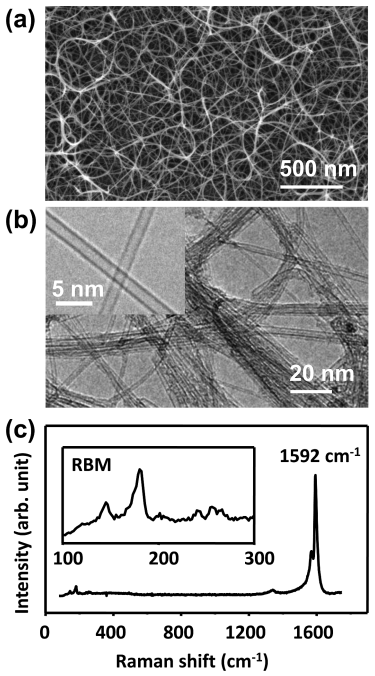

Figure 1. Characteristic (a) SEM and (b) TEM images of SWNTs synthesized by ACCVD. (c) Typical resonance Raman spectrum of a conventional ^{12}C SWNT film grown on a quartz substrate (488 nm excitation).

ethanol is decomposed at 800 °C for 0.1 s (a typical residual time in our CVD system with a 450 sccm ethanol flow rate), the gas composition at the furnace center would be approximately 90% ethanol plus a small percentage of ethylene. Though the experimentally measured decomposition is slightly slower than this calculation, the predicted concentration of various species agrees quite well. This implies that the real formation of SWNTs should be a competition among the original ethanol and ethanol-produced molecules. Considering the much smaller concentration of methane (same for CO) and its relatively lower activity, a quick speculation is the predominant contributors for the growth will be ethanol and ethylene. Acetylene is also a possible candidate due to its high efficiency, and was believed as one of the key molecules for SWNT growth. Therefore, whether SWNTs are always formed from ethylene/acetylene or if there is a direct contribution from ethanol remains an unanswered question, and serves as the starting point of this work.

Characterization of SWNTs Synthesized from Ethanol and Unequal Contribution of Two Atoms Revealed by Raman Spectroscopy. Figure 1a shows a typical scanning electron microscope (SEM) image of SWNTs synthesized on a quartz substrate using ACCVD. The transmission electron microscope (TEM) image in Figure 1b confirms that this method produced SWNTs with diameters ranging from 1 to 3 nm. No double-walled or multi-walled carbon nanotubes were observed. Figure 1c shows a characteristic resonance Raman spectrum

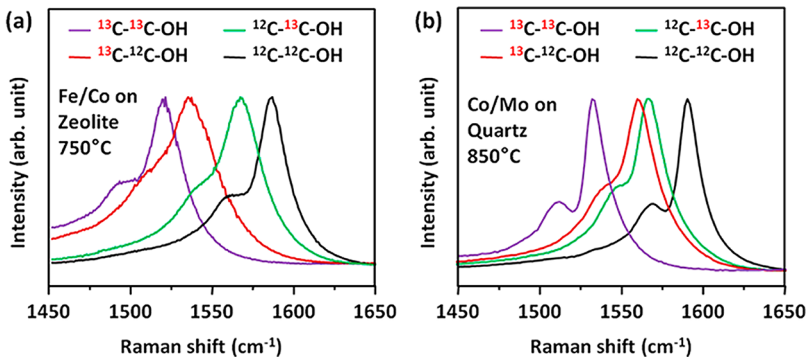

Figure 2. Raman spectra showing the G band of SWNTs grown from (a) Fe/Co supported by zeolite and (b) Co/Mo dip-coated onto quartz substrates (5 min reaction). Four different types of isotopically labeled ethanol yield four different Raman spectra, indicating that the two carbon atoms in an ethanol molecule are incorporated into the final SWNTs differently.

taken from the top of the SWNT film. The strong G peak and weak D peak clearly suggest high crystallinity of the SWNTs. When conventional ^{12}C ethanol is used for the growth, the produced SWNTs contain a negligible amount of ^{13}C (natural abundance is 1.1%) and the G peak locates at ~1592 cm^{-1}. However, when isotopically modified ethanol is used as the carbon source, the G peak shifts to lower frequency due to the enrichment of ^{13}C atoms.[28−30]

Figure 2 shows G band Raman spectra of SWNTs grown using four types of ethanol (^{12}C ethanol ($^{12}CH_3-{}^{12}CH_2-OH$), 1-^{13}C ethanol ($^{12}CH_3-{}^{13}CH_2-OH$), 2-^{13}C ethanol ($^{13}CH_3-{}^{12}CH_2-OH$), and 1,2-^{13}C ethanol ($^{13}CH_3-{}^{13}CH_2-OH$)) as carbon sources. Since the G band peak position is determined by the average in-plane vibration frequency of the C−C bonds in the graphitic lattice, the peak position can be used to determine the mean mass of the carbon atoms in the measured SWNTs.[29,31−33] Therefore, by labeling one of the carbons as ^{13}C, the contribution of a specific carbon atom in ethanol to the formation of a SWNT can also be determined. For example, when zeolite-supported Fe/Co (Figure 2a) is used at a CVD temperature of 750 °C, the G peak position of the SWNTs synthesized using 1-^{13}C ethanol and 2-^{13}C ethanol are very different, showing that one carbon atom (the no. 2 carbon, furthest away from the OH) is much more likely to be incorporated into the SWNT structure. However, the difference is much smaller in the case of Co/Mo catalyst on a quartz substrate at a higher CVD temperature (Figure 2b). The Raman spectra of SWNTs grown from 1-^{13}C ethanol and 2-^{13}C ethanol (red and green lines in Figure 2b) are very similar in this case, which means the contribution of the two carbon atoms is nearly equal (although the no. 2 carbon is still slightly preferred in the formation process). One direct conclusion from the imbalanced contribution of the two carbons is that, although an ethanol molecule may decompose into ethylene and further into acetylene at high temperature, these two symmetric molecules cannot be the only active precursors leading to SWNT formation. Particularly in the case when the incorporation of the no. 2 carbon is dominant, the contribution from symmetric molecules should be considered as insignificant. A preliminary consideration of the chemistry behind this difference is that, if the C−O bond in ethanol breaks (this could occur both in gas phase or on catalyst, as demonstrated later) and the C−C structure remains, the contribution of carbons 1 and 2 should be equal. However, if the C−C bond breaks predominantly, the resulting C and C−O would likely react much differently with the catalyst. More systematic investigations will be presented in the following, but in general, this strategy of isotope labeling may be used to trace the formation process from the carbon source to the final product and to discover some previously unnoticed effects that may not be easily accessible by conventional characterization methods.

Effect of CVD Temperature and Growth Substrate. A simpler case is presented in Figure 3, which shows Raman spectra of SWNTs grown at different temperatures. The samples are synthesized from dip-coated Co using silicon/SiO_2 (top) and quartz (bottom) as the substrates. Here we only compare the spectra of SWNTs from 1-^{13}C ethanol ($^{12}CH_3-{}^{13}CH_2-OH$), which is sufficient to calculate the contribution of both carbon atoms. A clear tendency observed is that the G peak shifts to lower energy as the growth temperature increases. This means the ratios of the two carbon atoms in SWNTs grown at 750, 800, and 850 °C are calculated to be approximately 15:85, 30:70, and 35:65, respectively. This suggests that at higher temperature the two carbon atoms in an ethanol molecule contribute more equally to SWNT formation.

The mechanism behind this tendency becomes straightforward when the thermal stability of ethanol is considered. Gas phase ethanol thermally decomposes at temperatures above 750 °C, producing primarily ethylene and water.[34,35] Since ethylene is known to be an efficient carbon precursor for SWNT growth,[10,17] it can also contribute to SWNT formation. Similarly, ethylene will further decompose at higher temperature and generate a small amount of acetylene in the gas phase. Even though the amount is small,

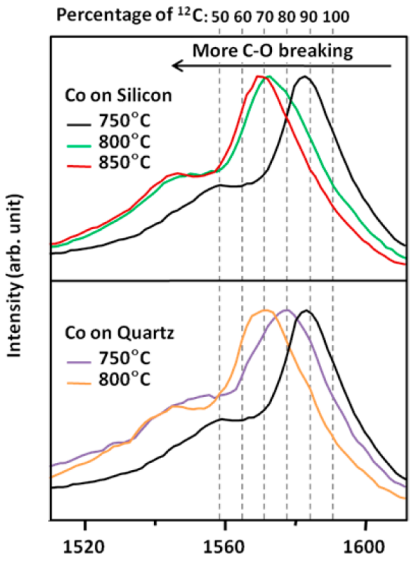

Figure 3. Raman spectra of SWNTs grown from dip-coated Co on a silicon/SiO_2 (top) and quartz (bottom) substrate at different temperatures indicate that the two carbon atoms in ethanol contribute more equally to SWNT formation at higher temperatures. The reaction period for all cases is 5 min.

highly efficient production of SWNTs from acetylene is known.[25] Therefore, multiple reaction pathways exist that result in SWNT formation. These pathways are indistinguishable under normal CVD conditions, but easily distinguishable when isotope-labeled ethanol is used. The difference between ethanol and ethylene/acetylene is that ethanol could yield SWNTs with an unequal ratio of ^{12}C:^{13}C, whereas the contribution from ethylene/acetylene—which has a symmetric structure—is expected to be equal. With this difference in mind, the cause for the temperature dependence of ^{13}C content in the final product becomes clear. At higher temperature (*e.g.*, 850 °C), the ethanol decomposes more quickly, thus more ethylene is present in the vicinity of the catalyst. This drives the 12C:13C contribution toward parity. At lower temperatures (*e.g.*, 750 °C), however, less ethanol decomposes before reaching the catalyst, thus the inequivalent contribution becomes more obvious. It is worth noting that even at 850 °C, the ^{12}C:^{13}C ratio is not 50:50, thus ethanol still works as the direct precursor. In our case, although a small amount of acetylene is generated, its contribution is less significant than the case reported by Zhong *et al.*,[26] where a much less active hydrocarbon CH_4 coexisted with acetylene. The detailed decomposition of ethanol at different temperatures is provided in the Supporting Information (Figure S1). In thermal decomposition, the C−O bond in an ethanol molecule breaks in the gas phase before the ethanol reaches the catalyst located on the substrate. Considering the no-flow CVD condition, the residual time of ethanol is much longer than in conventional CVD, so the thermal decomposition, that is, the contribution from the decomposed symmetric molecules should be largely overestimated. Therefore, we speculate that ethanol is still the primary carbon source in our conventional flow system. In principle, the contribution of different molecules can be estimated if their concentration and activity are known.

Some unexpected differences between silicon and quartz are noticed at 750 °C, as presented in Figure 3 (violet and black lines). SWNTs grown on quartz have a more equal contribution from the two carbon atoms than SWNTs grown on silicon. Specifically, the contribution from no. 1 and no. 2 carbons is 15:85 on Si but 20:80 on quartz. Following the previous discussion, a possible explanation of this trend is that quartz may decompose ethanol (possibly into ethylene/acetylene) by breaking the C−O bond of ethanol absorbed on its surface, thereby changing the local environment around the catalyst to a higher ethylene concentration. The contributions of decomposed molecules are enhanced, and a more equal contribution from the two carbon atoms is then observed in SWNTs synthesized on quartz relative to SWNTs synthesized on silicon. This difference between quartz and silicon clearly depicts that, in the catalyst formation of SWNT, the supporting material may be playing more significant and direct roles than previously thought. This may also be related to some previous puzzling observations where the quartz tube affects the CVD growth of CNTs.[36]

Effect of Mo on Decomposition of Ethanol and Its Possible Mechanism. The most pronounced difference is observed in the case of catalyst in the presence or absence of Mo. Molybdenum is often used as a subsidiary component in binary catalyst systems to improve the selectivity of SWNTs, as has been well demonstrated by the CoMoCAT and ACCVD processes. Since bulk Mo has a melting temperature of more than 2600 °C, the conventional understanding is that Mo can immobilize Co and prevent catalyst aggregation at high temperature.[37,38] Mo itself, however, is believed to be inefficient in producing SWNTs.[39] Regardless, SWNTs grown from 1-^{13}C ethanol on Co and Co/Mo catalysts have very different G peak positions. Figure 4a clearly shows that the addition of Mo into Co/Si catalyst makes ethanol grow SWNTs with a more balanced contribution of the two carbon atoms. At 750 °C, when Mo is absent, the ratio of no. 1 to no. 2 carbon is approximately 15:85 (because the thermal decomposition of ethanol is negligible at this temperature, we assume this value is near the intrinsic value for the SWNT-ethanol reaction in our system). When Mo is present, the contribution of no. 1/no. 2 carbons is changed significantly to be 32:68. One may consider this drastic change may arise from the change in catalyst size, since Mo addition is able to reduce the catalyst size significantly.[40] However, this possibility can be simply ruled out because, even for pure Co/Si, the catalyst has a similar size distribution and the

diameter range of the obtained SWNTs is 1−3 nm. No noticeable dependence on catalyst size is observed. Therefore, we believe this phenomenon provides experimental evidence that, in addition to the conventionally accepted role of immobilizing Co at high temperature, Mo also facilitates the formation of SWNTs by affecting the local environment around the catalyst and hence enhancing the possible reaction pathways.

One possible working mechanism for Mo is that $CoMoO_x$ is helping prevent oxidation of metallic Co.[38] Hence, the Co can have a stronger interaction with the incoming oxygen atom in the form of a C−C−O framework. This would likely promote C−O bond breaking on $CoMoO_x$ and even on a metallic Co cluster. Once the C−O is broken, the remaining C−C could be released back into the gas phase or directly used to form a SWNT; the contribution of the two carbons to the final product in this case would be equivalent. Another possible mechanism is that Mo can promote the disproportional reaction ($CO + CO \rightarrow C + CO_2$) on Co. In such case, the carbon in C−O has a chance to be incorporated into SWNTs. Although clarifying the very detailed mechanism cannot be fully accomplished at the present stage, the effect of Mo is clearly revealed in this study, and it always drives the contribution of ethanol's no. 1 and no. 2 carbons toward parity. The inequivalent contributions of the two carbons in the case of synthesis on Co/Si, Co/quartz, and Co/Mo/Si are summarized in Table 1.

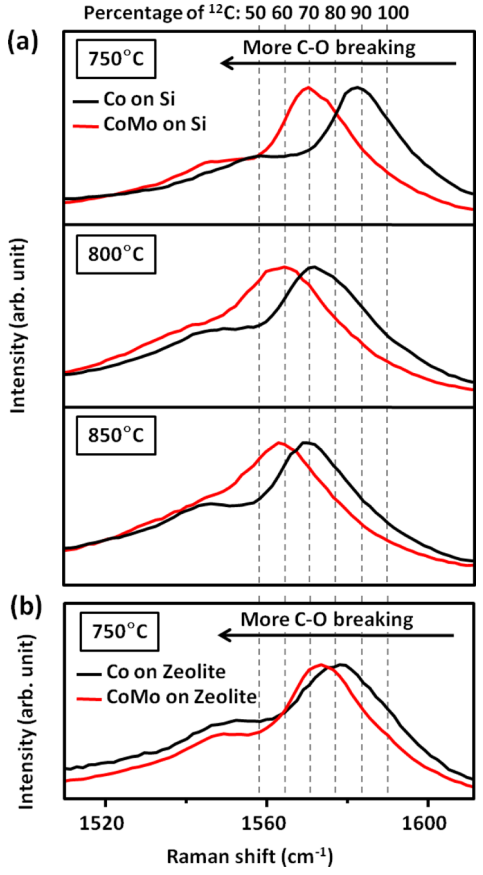

Figure 4. Raman spectra of SWNTs grown from dip-coated Co on silicon substrate at different temperatures with and without a subsidiary Mo component. Mo significantly affects the growth pathway of SWNTs, making the two carbon atoms in ethanol contribute more equally to the growth of SWNTs.

A similar trend is observed in the zeolite-supported Co catalyst system with and without Mo addition. As shown in Figure 4b, the presence of Mo leads to SWNTs with higher ^{13}C contribution, that is, the two carbon atoms are incorporating into the product more equally, which is consistent with the experiment of dip-coated Co catalyst on Si substrates. Meanwhile, if comparing the SWNTs obtained at 750 °C in Figure 4a and 4b, one can see that the effect of the zeolite support on ethanol decomposition is similar to that observed for Si and quartz substrates in Figure 3. This is also understandable because zeolite is a well-known catalyst in hydrogenation reactions.[41]

Semiquantitative Analysis of Gas-Phase and on-Surface Decomposition and Its Influence on SWNT Quality. Here we present a simplified model to summarize the above observations. There are four factors that affect the decomposition of a precursor molecule (here, ethanol) before forming a SWNT: (1) gas-phase thermal decomposition, (2) support-mediated decomposition, (3) Mo-caused preferential C−O breaking, (4) intrinsic breaking on Co sites. The first step occurs in the gas phase, and the latter three are most likely surface reactions. In this model, some ethanol may form SWNTs directly by reacting with Co particles (the active site), while some other ethanol may form SWNTs indirectly through an intermediate product such as ethylene or acetylene (either *via* gas-phase or on-surface decomposition routes). The sum product of these reaction pathways determines the SWNT end product. If thermal

TABLE 1. Ratios of Ethanol's no. 1/no. 2 Carbon Contribution to SWNTs Grown on Different Catalysts and at Different CVD Temperatures

	Co on Si			Co on quartz			Co/Mo on Si		
	750 °C	800 °C	850 °C	750 °C	800 °C	850 °C	750 °C	800 °C	850 °C
G peak position (cm^{-1})	1582.6	1576.6	1570.5	1576.6	1570.5	1567.5	1570.5	1564.5	1563.0
carbon no. 1:no. 2	15:85	30:70	35:65	20:80	32:68	37:63	32:68	40:60	45:55

TABLE 2. Estimate of the Percentage of Ethanol Decomposed at Different Stages[a]

	decomposition ratios at different temperatures		
catalyst type	750 °C	800 °C	850 °C
Co on Si	0:0:0:100	40:0:0:60	58:0:0:42
Co/Mo on Si	0:50:0:50	40:32:0:28	58:27:0:15
Co/Mo on zeolite	0:20:40:20	n/a	n/a

[a] The four values correspond to percentages of gas-phase decomposition, Mo-induced on-surface decomposition, support-induced on-surface decomposition, and active site determined intrinsic decomposition, respectively.

decomposition at 750 °C is neglected and it is assumed that the SWNTs obtained from Co/Si at 750 °C are produced by the intrinsic interaction between ethanol and Co, the percentage of ethanol decomposed *via* the above four stages may be quantified. A preliminary estimate is shown in Table 2. For Co/Mo dip-coated on Si at 750 °C, the gas-phase decomposition is negligible and the contribution of the two carbons are 15% and 85%. After the addition of Mo, the ratio changes to 32:68, suggesting Mo decomposes ~50% of the ethanol, possibly into ethylene—whose contribution of the two carbons would be 50:50—and water. Similarly, after comparing the Co/Si, Co/zeolite, and CoMo/zeolite, the percentage of ethanol decomposed by zeolite and Mo in a CoMo/zeolite system can be deduced to be 40% and 20%, respectively. On Co/Si at higher temperature, however, the gas-phase decomposition plays a more significant role, and is estimated to be ~40% at 800 °C and ~60% at 850 °C. In principle, changing the ethanol flow (i.e., ethanol residual time) will likely produce SWNTs with different contribution ratios and thus help to quantitatively confirm the role of thermal decomposition. However, due to the limited amount of expensive isotope-labeled ethanol, such an experiment is both technically and financially challenging at this stage.

These semi-quantitative estimates allow us to visualize how ethanol forms the final SWNT. Initially cool ethanol is heated to the reaction temperature before reaching the substrate or catalyst site. During this stage, ethanol may partially decompose into ethylene and water, depending on the temperature and elapsed time. After reaching the surface (not yet the catalyst itself), ethanol and the decomposed molecules diffuse through the catalyst support (in the case of porous powder-supported catalyst) and/or the already-formed SWNTs (particularly in the root growth of vertically aligned SWNTs) in order to reach the active site. Our previous study has shown that the inner channels are often smaller than the mean free path of the carbon source molecules,[42] thus during this stage the carbon-containing molecules are likely to collide with the sidewalls of existing SWNTs. Upon reaching the catalyst active site, both the catalyst (Co) and the supporting species (Mo or quartz substrate) are involved in the reaction chain, and various reaction pathways coexist and contribute to overall growth of SWNTs. One phenomenon generally observed in our process is that at high reaction temperature, when ethanol is thoroughly decomposed in the gas phase, the outer walls of produced SWNTs are often covered with a significant amount of amorphous carbon soot. When gas-phase thermal decomposition of ethanol is reduced, the SWNT walls are much cleaner. This is likely due to the more reactive products of thermal decomposition colliding with existing SWNTs. However, the decomposed product (such as ethylene and even some radicals) could be possibly more efficient for the growth,[25] so inhibiting gas-phase decomposition while enhancing on-surface decomposition is a possible way to increase the yield of clean, high-quality SWNTs. A schematic showing the whole journey of an ethanol molecule during CVD formation of SWNTs is presented in Figure 5.

Finally, we briefly discuss the origin of the very imbalanced contribution of ethanol's two carbon atoms happening at an active site (e.g., no. 2 carbon is 85% incorporated at 750 °C on Co/Si). When an ethanol molecule reaches an active Co site, one possible mechanism for the preferred incorporation of the no. 2 carbon (the one away from the OH) is that the C−C bond in CH_3-CH_2-OH breaks. In this process, the no. 2 C remains while the no. 1 C is released together with the C−O group into the gas phase. Therefore, the chemistry in this model is that ethanol dissociates, with the no. 2 C being incorporated into the catalyst hence into the SWNT. The no. 1 carbon can be released as methanol or CO, or two no. 1 carbons can meet on the surface and undergo the disproportional reaction ($CO + CO \rightarrow C + CO_2$) to release CO_2. The released methanol and CO may come back to the catalyst and have another chance to undergo the disproportional reaction (CO and methanol are known as efficient carbon sources in some systems), causing the sequential incorporation of the no. 1 carbon. No matter which case, if all original C−O structures are involved, the no. 2 carbon concentration will be strictly 2/3 (67%). However, in our system the disproportional reaction is less favored, and both methanol and CO are much less active than ethanol, thus the secondary incorporation of no. 1 is unlikely. The clear preference for the no. 2 carbon supports this model, because 85% contribution means that less than 17% of the released no. 1 carbon is incorporated. The real case should be even less than 17%, since we cannot rule out the possibility that ethanol could dissociate the no. 1 and no. 2 carbons simultaneously (the C−O bond breaks) by releasing H_2O and H_2. A collection showing all decomposition pathways of ethanol in the gas phase and on the catalyst surface, as well as the resulting ratio of no. 1 and no. 2 carbons incorporated in SWNTs is

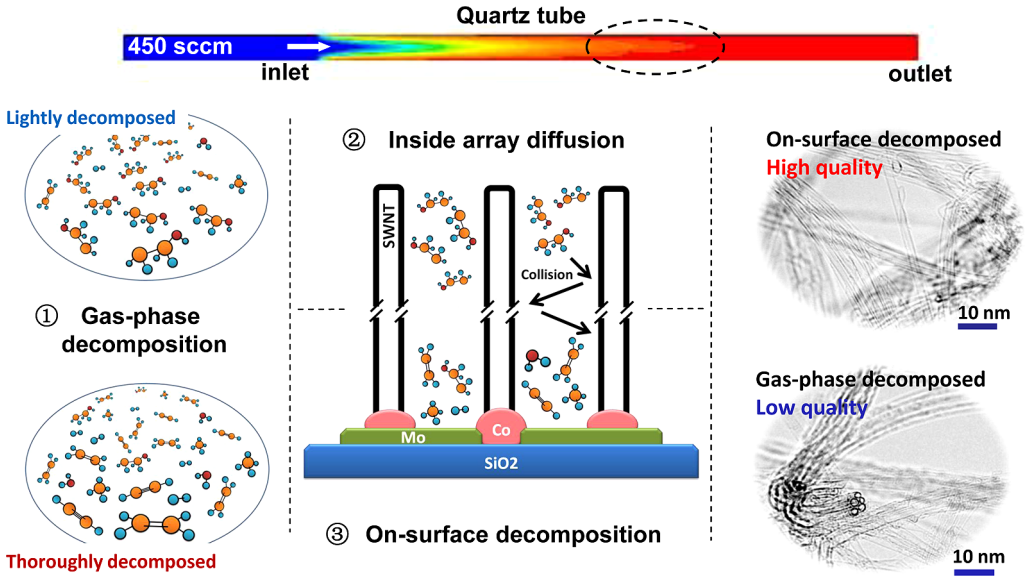

Figure 5. Ethanol decomposition and SWNT quality. Ethanol may undergo gas-phase decomposition, array diffusion and on-surface reaction, among which we confirm both catalyst support and some secondary metal species such as Mo contribute to this heterogeneous reaction. The quality of obtained SWNTs is strongly affected by the stage at which the ethanol is decomposed.

presented in Supporting Information, Figure S5. In this model, the incorporation of the less-preferred carbon atom (no. 1 carbon) should be possible either sequentially or simultaneously. In all our experiments no preferred incorporation of the no. 1 carbon is observed. This is understandable because the no. 1 carbon can be preferentially lost when the C−C bond breaks at any stage. The selectivity/competition between C−C breaking or C−O breaking should be also related to properties of the active site. Some previous DFT calculations revealed preferred reaction pathways for carbon precursors interacting with different metals.[43,44] For example, Irle *et al.* claimed that on Co, the C−C bond is easily broken, whereas the C−O dissociates with higher probability on Ni.[45] This seems to be consistent with the trend observed in our experiments. We also tried the growth on zeolite-supported Fe, Co, and Ni catalyst and observed a clear difference (Supporting Information, Figure S4), but further theoretical and experimental investigations are needed to examine how the type of active sites, for example, Fe, Co, Ni, and other factors may affect this reaction.

CONCLUSIONS

To summarize, we propose a novel strategy to identify the contributions from the two different carbons in ethanol to SWNT formation by using isotopically modified ethanol as the carbon source. The no. 2 carbon was found to always be incorporated into the product more preferentially (up to 85%) than the no. 1 carbon, which confirms the direct interaction between the ethanol and catalyst. Also, the strong parameter-dependent inequivalent incorporation of carbon atoms clearly reveals that the supporting/secondary species in the catalyst (such as Mo), as well as the catalyst support substrate, are directly involved in the reaction chain and strongly influence the decomposition of ethanol. These preliminary results may motivate further discussion on the details of the SWNT growth mechanism, and help to improve control over the quality of SWNTs.

EXPERIMENTAL SECTION

SWNTs were synthesized by ACCVD using ethanol as the carbon source. The uniqueness of the present work is that, instead of conventional ethanol, ^{13}C labeled ethanol was used, that is, $^{12}CH_3-^{13}CH_2-OH$ (1-^{13}C ethanol) and $^{13}CH_3-^{12}CH_2-OH$ (2-^{13}C ethanol). The average mass of the carbon atoms in the synthesized SWNT was evaluated by Raman spectroscopy, which reveals the relative contribution of carbon isotopes in the final product. Zeolite-supported Co, Co/Mo, and dip-coated Co, Co/Mo on silicon or quartz substrates were used for SWNT growth. More details of the catalyst preparation process and CVD parameters can be found in our previous reports.[14,25,46,47] All CVD experiments were performed in a furnace (inner diameter, 26 mm; heating zone ≈ 80 cm) using a no-flow CVD condition, meaning a fixed amount of ethanol was introduced into the chamber with both ends sealed in order to efficiently use the expensive isotope-labeled ethanol.[28] The decomposition of ethanol along with the residual time in a no-flow condition calculated using the FLUENT software package is presented as Supporting Information, Figure S2. The ethanol pressure is 1.3 kPa and CVD reaction period is 5 min unless described otherwise. The as-obtained materials were characterized by scanning electron microscopy (SEM, Hitachi S-4800), and transmission electron microscopy (TEM, JEOL 2000EXII operated at 120 kV). The concentration of ethanol and other decomposed species was calculated by Chemkin with the chemical reaction model proposed by Marinov,[48] and experimentally measured using Fourier transform infrared spectroscopy (FTIR). All Raman spectra were taken from the sample

top using a 488 nm excitation laser. Obtaining Raman spectra from several points along the cross-section of the array reveals a slight shift in G peak position from the tip to the root of the array, but spectra obtained from the top of the array well averages these values, and the obtained G peak position is shifted by less than 2 cm^{-1} from the value at the tip of the array (Supporting Information, Figure S6). Spectra were obtained using different objective lenses, laser power, and gratings to avoid laser heating[49] and ensure sufficient resolution; one SWNT film was also checked to confirm uniformity (Supporting Information, Figure S7).

Conflict of Interest: The authors declare no competing financial interest.

Acknowledgment. Part of this work was financially supported by Grant-in-Aid for Scientific Research (22226006, 23760179, and 23760180), JSPS Core-to-Core Program, the "Global Center for Excellence for Mechanical Systems Innovation" program at the University of Tokyo, National Science Foundation of China (51002190), Guangdong Provincial Natural Science Foundation of China (2011040004714), and by the open funds of State Key Laboratory of Optoelectronic Materials and Technologies.

Supporting Information Available: Thermal decomposition of ethanol at 750, 800, and 850 °C; full Raman spectra of SWNTs obtained on Co/Si catalyst at 750, 800, and 850 °C with and without Mo addition using 1-^{13}C ethanol as the carbon source; Raman spectra of SWNTs obtained on zeolite supported Fe, Co, Ni catalyst grown at 750 °C using 1-^{13}C ethanol as the carbon source; Schematics of reaction pathway and resulting ratio of no. 1 and no. 2 carbon incorporated in SWNTs; cross-sectional Raman spectra of vertically aligned SWNT array; Raman spectra of a standard ^{12}C SWNT sample measured with different lens and laser power; Raman spectra of a ^{13}C-enriched SWNT sample taken at different sites; Raman spectra of a standard ^{12}C SWNT sample measured with different gratings of the monochromator. This material is available free of charge *via* the Internet at http://pubs.acs.org.

REFERENCES AND NOTES

1. Dai, H.; Rinzler, A. G.; Nikolaev, P.; Thess, A.; Colbert, D. T.; Smalley, R. E. Single-Wall Nanotubes Produced by Metal-Catalyzed Disproportionation of Carbon Monoxide. *Chem. Phys. Lett.* **1996**, *260*, 471–475.
2. Sinnott, S. B.; Andrews, R.; Qian, D.; Rao, A. M.; Mao, Z.; Dickey, E. C.; Derbyshire, F. Model of Carbon Nanotube Growth through Chemical Vapor Deposition. *Chem. Phys. Lett.* **1999**, *315*, 25–30.
3. Reina, A.; Jia, X. T.; Ho, J.; Nezich, D.; Son, H. B.; Bulovic, V.; Dresselhaus, M. S.; Kong, J. Large Area, Few-Layer Graphene Films on Arbitrary Substrates by Chemical Vapor Deposition. *Nano Lett.* **2009**, *9*, 30–35.
4. Li, X. S.; Cai, W. W.; An, J. H.; Kim, S.; Nah, J.; Yang, D. X.; Piner, R.; Velamakanni, A.; Jung, I.; Tutuc, E.; *et al.* Large-Area Synthesis of High-Quality and Uniform Graphene Films on Copper Foils. *Science* **2009**, *324*, 1312–1314.
5. Cassell, A. M.; Raymakers, J. A.; Kong, J.; Dai, H. J. Large Scale CVD Synthesis of Single-Walled Carbon Nanotubes. *J. Phys. Chem. B* **1999**, *103*, 6484–6492.
6. Murakami, Y.; Miyauchi, Y.; Chiashi, S.; Maruyama, S. Characterization of Single-Walled Carbon Nanotubes Catalytically Synthesized from Alcohol. *Chem. Phys. Lett.* **2003**, *374*, 53–58.
7. Dupuis, A. C. The Catalyst in the CCVD of Carbon Nanotubes—A Review. *Prog. Mater. Sci.* **2005**, *50*, 929–961.
8. Moisala, A.; Nasibulin, A. G.; Kauppinen, E. I. The Role of Metal Nanoparticles in the Catalytic Production of Single-Walled Carbon Nanotubes—A Review. *J. Phys.: Condens. Matter* **2003**, *15*, S3011–S3035.
9. Chiang, W. H.; Sankaran, R. M. Linking Catalyst Composition to Chirality Distributions of As-Grown Single-Walled Carbon Nanotubes by Tuning Ni_xFe_{1-x} Nanoparticles. *Nat. Mater.* **2009**, *8*, 882–886.
10. Hafner, J. H.; Bronikowski, M. J.; Azamian, B. R.; Nikolaev, P.; Rinzler, A. G.; Colbert, D. T.; Smith, K. A.; Smalley, R. E. Catalytic Growth of Single-Wall Carbon Nanotubes from Metal Particles. *Chem. Phys. Lett.* **1998**, *296*, 195–202.
11. Su, M.; Zheng, B.; Liu, J. A Scalable CVD Method for the Synthesis of Single-Walled Carbon Nanotubes with High Catalyst Productivity. *Chem. Phys. Lett.* **2000**, *322*, 321–326.
12. Li, Y.; Liu, J.; Wang, Y. Q.; Wang, Z. L. Preparation of Monodispersed Fe−Mo Nanoparticles as the Catalyst for CVD Synthesis of Carbon Nanotubes. *Chem. Mater.* **2001**, *13*, 1008–1014.
13. Cui, H.; Eres, G.; Howe, J. Y.; Puretkzy, A.; Varela, M.; Geohegan, D. B.; Lowndes, D. H. Growth Behavior of Carbon Nanotubes on Multilayered Metal Catalyst Film in Chemical Vapor Deposition. *Chem. Phys. Lett.* **2003**, *374*, 222–228.
14. Murakami, Y.; Chiashi, S.; Miyauchi, Y.; Hu, M. H.; Ogura, M.; Okubo, T.; Maruyama, S. Growth of Vertically Aligned Single-Walled Carbon Nanotube Films on Quartz Substrates and Their Optical Anisotropy. *Chem. Phys. Lett.* **2004**, *385*, 298–303.
15. Bachilo, S. M.; Balzano, L.; Herrera, J. E.; Pompeo, F.; Resasco, D. E.; Weisman, R. B. Narrow (*n*,*m*)-Distribution of Single-Walled Carbon Nanotubes Grown Using a Solid Supported Catalyst. *J. Am. Chem. Soc.* **2003**, *125*, 11186–11187.
16. Maruyama, S.; Kojima, R.; Miyauchi, Y.; Chiashi, S.; Kohno, M. Low-Temperature Synthesis of High-Purity Single-Walled Carbon Nanotubes from Alcohol. *Chem. Phys. Lett.* **2002**, *360*, 229–234.
17. Hata, K.; Futaba, D. N.; Mizuno, K.; Namai, T.; Yumura, M.; Iijima, S. Water-Assisted Highly Efficient Synthesis of Impurity-Free Single-Walled Carbon Nanotubes. *Science* **2004**, *306*, 1362–1364.
18. Noda, S.; Hasegawa, K.; Sugime, H.; Kakehi, K.; Zhang, Z.; Maruyama, S.; Yamaguchi, Y. Millimeter-Thick Single-Walled Carbon Nanotube Forests: Hidden Role of Catalyst Support. *Jpn. J. Appl. Phys.* **2007**, *46*, 399–401.
19. Zhong, G. F.; Warner, J. H.; Fouquet, M.; Robertson, A. W.; Chen, B. A.; Robertson, J. Growth of Ultrahigh Density Single-Walled Carbon Nanotube Forests by Improved Catalyst Design. *ACS Nano* **2012**, *6*, 2893–2903.
20. Geohegan, D. B.; Puretzky, A. A.; Jackson, J. J.; Rouleau, C. M.; Eres, G.; More, K. L. Flux-Dependent Growth Kinetics and Diameter Selectivity in Single-Wall Carbon Nanotube Arrays. *ACS Nano* **2011**, *5*, 8311–8321.
21. Zheng, L. X.; O'Connell, M. J.; Doorn, S. K.; Liao, X. Z.; Zhao, Y. H.; Akhadov, E. A.; Hoffbauer, M. A.; Roop, B. J.; Jia, Q. X.; Dye, R. C.; *et al.* Ultralong Single-Wall Carbon Nanotubes. *Nat. Mater.* **2004**, *3*, 673–676.
22. Murakami, Y.; Miyauchi, Y.; Chiashi, S.; Maruyama, S. Direct Synthesis of High-Quality Single-Walled Carbon Nanotubes on Silicon and Quartz Substrates. *Chem. Phys. Lett.* **2003**, *377*, 49–54.
23. Eres, G.; Kinkhabwala, A. A.; Cui, H. T.; Geohegan, D. B.; Puretzky, A. A.; Lowndes, D. H. Molecular-Beam-Controlled Nucleation and Growth of Vertically Aligned Single-Wall Carbon Nanotube Arrays. *J. Phys. Chem. B* **2005**, *109*, 16684–16694.
24. Eres, G.; Rouleau, C. M.; Yoon, M.; Puretzky, A. A.; Jackson, J. J.; Geohegan, D. B. Model for Self-Assembly of Carbon Nanotubes from Acetylene Based on Real-Time Studies of Vertically Aligned Growth Kinetics. *J. Phys. Chem. C* **2009**, *113*, 15484–15491.
25. Xiang, R.; Einarsson, E.; Okawa, J.; Miyauchi, Y.; Maruyama, S. Acetylene-Accelerated Alcohol Catalytic Chemical Vapor Deposition Growth of Vertically Aligned Single-Walled Carbon Nanotubes. *J. Phys. Chem. C* **2009**, *113*, 7511–7515.
26. Zhong, G.; Hofmann, S.; Yan, F.; Telg, H.; Warner, J. H.; Eder, D.; Thomsen, C.; Milne, W. I.; Robertson, J. Acetylene: A Key Growth Precursor for Single-Walled Carbon Nanotube Forests. *J. Phys. Chem. C* **2009**, *113*, 17321–17325.
27. Sugime, H.; Noda, S. Cold-Gas Chemical Vapor Deposition To Identify the Key Precursor for Rapidly Growing Vertically-Aligned Single-Wall and Few-Wall Carbon Nanotubes from Pyrolyzed Ethanol. *Carbon* **2012**, *50*, 2953–2960.

28. Liu, L.; Fan, S. S. Isotope Labeling of Carbon Nanotubes and Formation of $^{12}C-^{13}C$ Nanotube Junctions. *J. Am. Chem. Soc.* **2001**, *123*, 11502–11503.
29. Simon, F.; Kramberger, C.; Pfeiffer, R.; Kuzmany, H.; Zolyomi, V.; Kürti, J.; Singer, P. M.; Alloul, H. Isotope Engineering of Carbon Nanotube Systems. *Phys. Rev. Lett.* **2005**, *95*, 017401.
30. Xiang, R.; Zhang, Z. Y.; Ogura, K.; Okawa, J.; Einarsson, E.; Miyauchi, Y.; Shiomi, J.; Maruyama, S. Vertically Aligned ^{13}C Single-Walled Carbon Nanotubes Synthesized by No-Flow Alcohol Chemical Vapor Deposition and Their Root Growth Mechanism. *Jpn. J. Appl. Phys.* **2008**, *47*, 1971–1974.
31. Dresselhaus, M. S.; Dresselhaus, G.; Saito, R.; Jorio, A. Raman Spectroscopy of Carbon Nanotubes. *Phys. Rep.-Rev., Sec. Phys. Lett.* **2005**, *409*, 47–99.
32. Costa, S. D.; Fantini, C.; Righi, A.; Bachmatiuk, A.; Rümmeli, M. H.; Saito, R.; Pimenta, M. A. Resonant Raman Spectroscopy on Enriched ^{13}C Carbon Nanotubes. *Carbon* **2011**, *49*, 4719–4723.
33. Zhao, P.; Einarsson, E.; Xiang, R.; Murakami, Y.; Chiashi, S.; Shiomi, J.; Maruyama, S. Isotope-Induced Elastic Scattering of Optical Phonons in Individual Suspended Single-Walled Carbon Nanotubes. *Appl. Phys. Lett.* **2011**, *99*, 093104.
34. Rotzoll, G. High-Temperature Pyrolysis of Ethanol. *J. Anal. Appl. Pyrol.* **1985**, *9*, 43–52.
35. Hou, B.; Xiang, R.; Inoue, T.; Einarsson, E.; Chiashi, S.; Shiomi, J.; Miyoshi, A.; Maruyama, S. Decomposition of Ethanol and Dimethyl Ether during Chemical Vapor Deposition Synthesis of Single-Walled Carbon Nanotubes. *Jpn. J. Appl. Phys.* **2011**, *50*, 065101.
36. Liu, K.; Liu, P.; Jiang, K.; Fan, S. S. Effect of Carbon Deposits on the Reactor Wall During the Growth of Multi-walled Carbon Nanotube Arrays. *Carbon* **2007**, *45*, 2379–2387.
37. Herrera, J. E.; Balzano, L.; Borgna, A.; Alvarez, W. E.; Resasco, D. E. Relationship between the Structure/Composition of Co–Mo Catalysts and their Ability to Produce Single-Walled Carbon Nanotubes by CO Disproportionation. *J. Catal.* **2001**, *204*, 129–145.
38. Hu, M. H.; Murakami, Y.; Ogura, M.; Maruyama, S.; Okubo, T. Morphology and Chemical State of Co–Mo Catalysts for Growth of Vertically Aligned Single-Walled Carbon Nanotubes on Quartz Substrates. *J. Catal.* **2004**, *225*, 230–239.
39. Yoshida, H.; Shimizu, T.; Uchiyama, T.; Kohno, H.; Homma, Y.; Takeda, S. Atomic-Scale Analysis on the Role of Molybdenum in Iron-Catalyzed Carbon Nanotube Growth. *Nano Lett.* **2009**, *9*, 3810–3815.
40. Xiang, R.; Einarsson, E.; Murakami, Y.; Shiomi, J.; Chiashi, S.; Tang, Z. K.; Maruyama, S. Diameter Modulation of Vertically Aligned Single-Walled Carbon Nanotubes. *ACS Nano* **2012**, *6*, 7472.
41. Subramani, V.; Gangwal, S. K. A Review of Recent Literature to Search for an Efficient Catalytic Process for the Conversion of Syngas to Ethanol. *Energy Fuel* **2008**, *22*, 814–839.
42. Xiang, R.; Yang, Z.; Zhang, Q.; Luo, G. H.; Qian, W. Z.; Wei, F.; Kadowaki, M.; Einarsson, E.; Maruyama, S. Growth Deceleration of Vertically Aligned Carbon Nanotube Arrays: Catalyst Deactivation or Feedstock Diffusion Controlled? *J. Phys. Chem. C* **2008**, *112*, 4892–4896.
43. Yazyev, O. V.; Pasquarello, A. Effect of Metal Elements in Catalytic Growth of Carbon Nanotubes. *Phys. Rev. Lett.* **2008**, *100*, 156102.
44. Irle, S.; Ohta, Y.; Okamoto, Y.; Page, A. J.; Wang, Y.; Morokuma, K. Milestones in Molecular Dynamics Simulations of Single-Walled Carbon Nanotube Formation: A Brief Critical Review. *Nano Res.* **2009**, *2*, 755–767.
45. Page, A. J.; Ohta, Y.; Irle, S.; Morokuma, K. Mechanisms of Single-Walled Carbon Nanotube Nucleation, Growth, and Healing Determined Using QM/MD Methods. *Acc. Chem. Res.* **2010**, *43*, 1375–1385.
46. Igarashi, H.; Murakami, H.; Murakami, Y.; Maruyama, S.; Nakashima, N. Purification and Characterization of Zeolite-Supported Single-Walled Carbon Nanotubes Catalytically Synthesized from Ethanol. *Chem. Phys. Lett.* **2004**, *392*, 529–532.
47. Xiang, R.; Wu, T. Z.; Einarsson, E.; Suzuki, Y.; Murakami, Y.; Shiomi, J.; Maruyama, S. High-Precision Selective Deposition of Catalyst for Facile Localized Growth of Single-Walled Carbon Nanotubes. *J. Am. Chem. Soc.* **2009**, *131*, 10344–10345.
48. Marinov, N. M. A Detailed Chemical Kinetic Model for High Temperature Ethanol Oxidation. *Int. J. Chem. Kinet.* **1999**, *31*, 183–220.
49. Chiashi, S.; Murakami, Y.; Miyauchi, Y.; Maruyama, S. Temperature Dependence of Raman Scattering from Single-walled Carbon Nanotubes - Undefined Radial Breathing Mode Peaks at High Temperatures. *Jpn. J. Appl. Phys.* **2008**, *47*, 2010–2015.